Full-f and δf gyrokinetic particle simulations of Alfvén waves and energetic particle physics

Z.X. Lu, G. Meng, R. Hatzky, Ph. Lauber, M. Hoelzl; NL collision w/ input from A. Chankin, G. Meng, A. Bergmann …

[Lu, et al, Plasma Phys. Control. Fusion, 65, 034004 (2023)]

Acknowledge: A. Mishchenko, ORB5, EUTERPE, JOREK groups, L. Rekhviashvili, E. Sonnendrücker, F. Zonca

TSVV8; ACH/MPG01; ATEP/NLED ENR; TSVV10 projects

TSVV10 meeting, 17th April 2023

This work has been carried out within the framework of the EUROfusion Consortium, funded by the European Union via the Euratom Research and Training Programme (Grant Agreement No 101052200 — EUROfusion). Views and opinions expressed are however those of the author(s) only and do not necessarily reflect those of the European Union or the European Commission. Neither the European Union nor the European Commission can be held responsible for them.

Connection & possible contribution to TSVV10 from TRIMEG (previously/currently participated in TSVV8)

(Mixed δf)-full f scheme electromagnetic particle models

- Mixed variables/pullback scheme in full f
- Marker loading using constants of motion in full f model

Full f nonlinear collision operator using Rosenbluth potential

Field-aligned finite element method for multiple-n nonlinear simulations

Recap: Triangular mesh based gyrokinetic code

Structured mesh

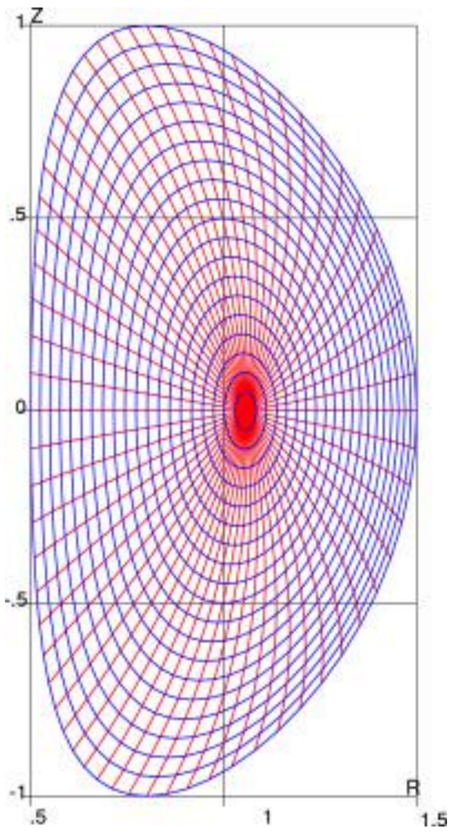

GTC,GTS,GEM
MEGA, HMGC
LIGKA, HAGIS
NOVA, JOREK

STRUPHY

TRIMEG-GKX

- **Unstructured mesh**

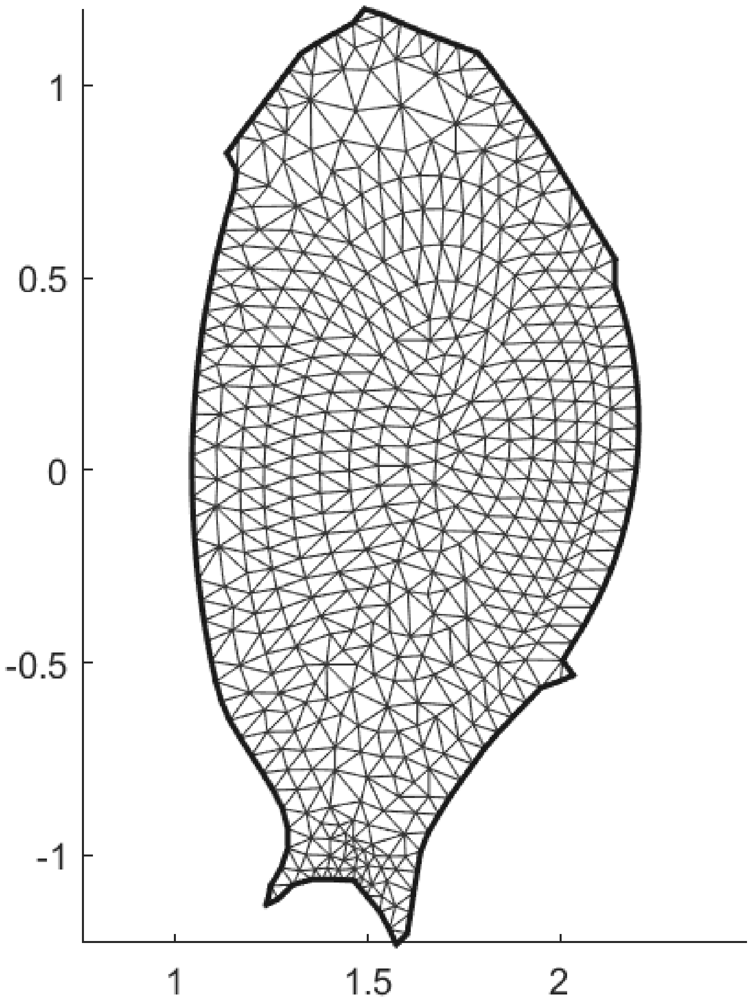

XGC, M3D(-C1)

TRIMEG-C0/C1

Recap: Development of TRIMEG code and Physics studies

TRIangular MEsh based Gyrokinetic code

Aiming for physics studies with X point, EM and kinetic electrons

Before 2019:electrostatic model, explicit scheme, δf (low noise, fast), (R,Z) coordinate, unstructured mesh, mixed particle-in-cell-particle-in-Fourier

[Z.X. Lu, Ph. Lauber, T. Hayward-Schneider, A. Bottino, M. Hoelzl, Phys. Plasmas , 26, 122503 (2019)]

2019-2021:electromagnetic, implicit scheme, full f, "eXtended" to structured mesh in a test version, realistic mass ratio, multiple species

[Z.X. Lu, G. Meng, M. Hoelzl, Ph. Lauber, Journal Comput. Phys. 440 (2021) 110384]

Recent work

- Numerical improvement
  - High order finite element in both structured/unstructured meshes
  - Control Variate and noise reduction

[Lu, Meng, Hatzky, Hoelzl, Lauber, PPCF (2023)]

- Neoclassical physics
  - Electron transport, bootstrap current

[L. Rekhviashvili, master thesis, TRIMEG-C0]

  - Neoclassical Er

- Physics studies related to AUG, benchmark with LIGKA, HMGC

[Meng, Lauber, Wang, Lu, Plasma Science Tech 025101 (2022)]

- Chen, Zonca et al. GK-E&B
  - GK-E&B is a powerful model suitable for multi-scale physics
  - Test in TRIMEG shows GK-E&B's capability for small d_e

[Rosen, Lu, Hoelzl, Phys. Plasmas, 022502 (2022)]

Recap: ITG simulations in TRIMEG

ITG mode is simulated in the whole plasma volume

- **Experimental magnetic equilibrium**
- **Analytical density, temperature profiles**
- **Dominant terms in equations of motion**
- **Linear/nonlinear ITG simulations demonstrate the capability of the unstructured mesh in treating the whole plasma volume**

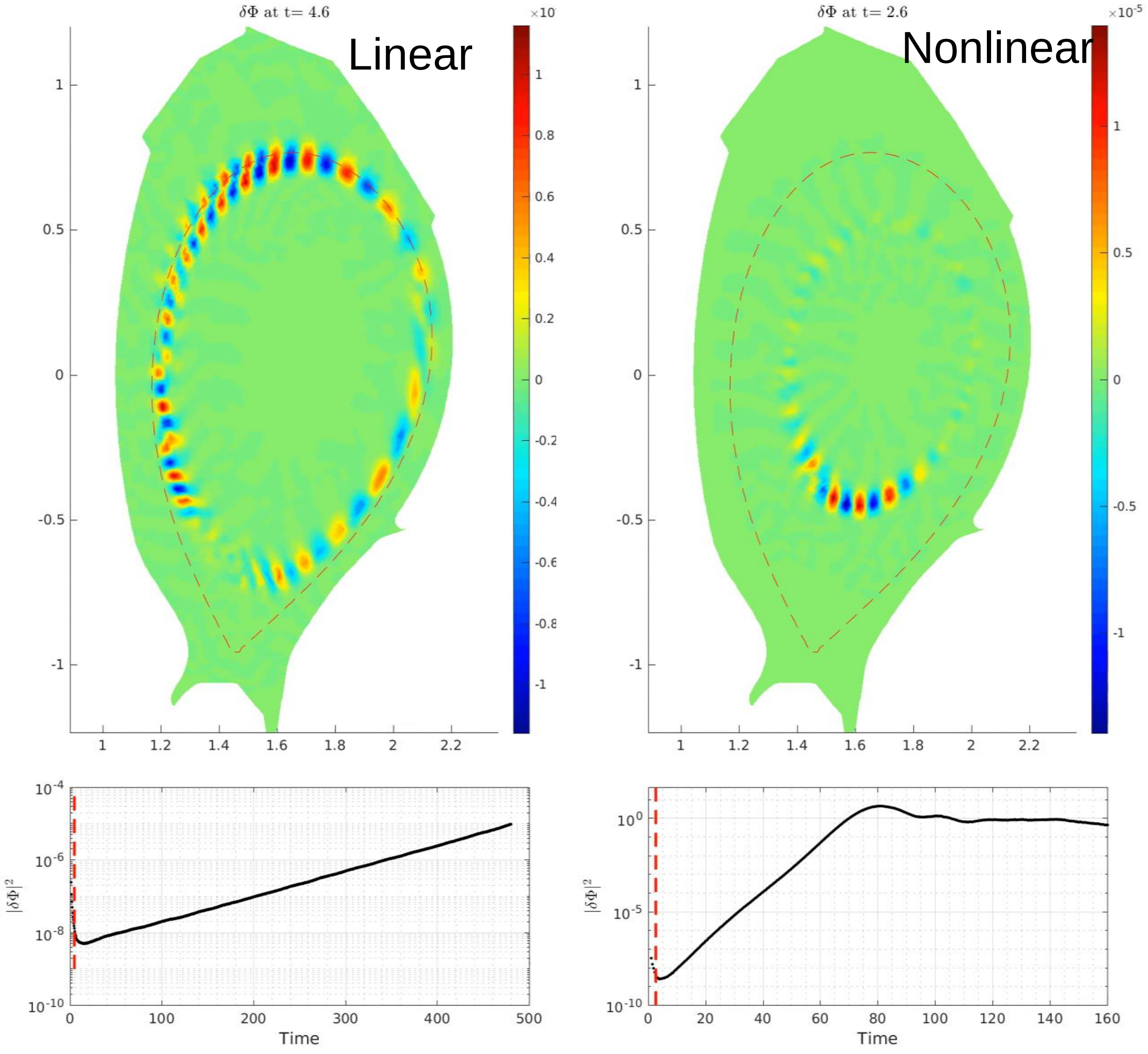

[Z.X. Lu, Ph. Lauber, T. Hayward-Schneider, A. Botti M. Hoelzl, *Phys. Plasmas* , 26, 122503 (2019)]

Full f simulations of Alfvén waves and energetic particle physics

Origin of the challenge in gyrokinetic electromagnetic simulations

$$p_\parallel = v_\parallel + \frac{q_s}{m_s}\delta A_\parallel$$

- $v_\parallel$ **form:** $\partial\delta A_\parallel/\partial t$ **needs implicit treatment.**
- $p_\parallel$ **form: Cancellation problem (for** $\nabla_\perp^2 < \frac{1}{d_e^2}$**).**
- **In full f scheme, high noise, synergy from neoclassical physics bring in more challenges**

$$\frac{dv_\parallel}{dt} = -\left(\boldsymbol{b}\cdot\nabla\delta\phi + \frac{\partial}{\partial t}\delta A_\parallel\right);\ \nabla_\perp^2\delta A_\parallel = C_A\delta j_{\parallel,v_\parallel}$$

$$\frac{dp_\parallel}{dt} = -\boldsymbol{b}\cdot\nabla(\delta\phi - v_\parallel\delta A_\parallel);\ (\nabla_\perp^2 - \frac{1}{d_e^2})\delta A_\parallel = C_A\delta j_{\parallel,p_\parallel}$$

	Full f	**Direct δf**	Traditional δf
$v_\parallel$	Implicit: Lu21JCP		Implicit: Sturdevant 19APS/21POP, XGC
$p_\parallel$	Exercise in 2021 (good in filter-free capability; full f)	Hatzky19	Mishchenko04/05; Bottino11, Hatzky19, this work
Mixed variable/Pull back	this work; XGC (Hager2022)	Hatzky19; TRIMEG exercise in 2021	Mischchenko18, Cole21 (XGC), Hatzky19, this work

Recent work: explicit scheme, full f and δf on the same footing

Focus on $p_{\|}$ form, instead of $v_{\|}$ form

Noise reduction in full f or mixed δf-full f schemes

Good description of energetic particles in full f simulations

[Lu, Meng, Hatzky, Hoelzl, Lauber, PPCF (2023)]

Essence of the constant of motion in EP description: PSZS (phase space zonal structure)

[Zonca et al, New J. Phys. 17, 013052 (2015)
Falessi et al, Phys. Plasmas, 26, 022305 (2019)

The mixed variable/pullback scheme and the iterative $p_\parallel$ scheme

Gyrokinetic model with mixed variables: $\delta A_\parallel = \delta A_\parallel^{\rm s} + \delta A_\parallel^{\rm h}$, $u_\parallel = v_\parallel + \frac{q_s}{m_s}\delta A_\parallel^{\rm h}$

1. **Quasi-neutrality equation:** $-\nabla \cdot \left(\frac{q_s n_{0s}}{B\omega_{cs}}\nabla_\perp \delta\phi\right) = \sum_s q_s \delta n_s$
2. **Parallel Ampere's law:** $\left(\nabla_\perp^2 - \sum_s \frac{1}{d_s^2}\right)\delta A_{\parallel,0}^{\rm h} = -\nabla_\perp^2 \delta A_\parallel^{\rm s} - \mu_0 \delta j_\parallel$
3. **Iterative Ampere solver:** $\left(\nabla_\perp^2 - \sum_s \frac{1}{d_s^2}\right)\delta A_{\parallel,p}^{\rm h} = \sum_s \left(\frac{G_s}{d_s^2} - \frac{1}{d_s^2}\right)\delta A_{\parallel,p-1}^{\rm h}$, $p = 1,2,\ldots$
4. **Ohm's law:** $\partial_t \delta A_\parallel^{\rm s} + \partial_\parallel \delta\phi = 0$
5. **Fourier filter (Particle-in-Fourier for moment, matrix inverse for field)**
6. **Guiding center's equations of motion, weight equation for δf & full f also derived**
7. **Reduction to pure $p_\parallel$ form (improved):** $\delta A_\parallel^{\rm s} = 0$
   - MV-PB implemented for δf (Mishchenko et. al.);
   - Full f MV-PB discussed in Hatzky19; not implemented before (XGC: simplified w/o iterative Ampere's law, Hager2022)

- Goal: $\nabla_\perp^2 \delta A_\parallel^{\rm h} - \sum_s \frac{G_s}{d_s^2} A_\parallel^{\rm h} = -\nabla_\perp^2 \delta A_\parallel^{\rm s} - \mu_0 \delta j_\parallel$;
- $\frac{G_s}{d_s^2} A_\parallel^{\rm h}$: accurate adiabatic part
- $G_s \rightarrow 1$ in analytical limit

Discretization from marker to physical distribution: full f versus δf

Full f scheme

For N markers with given distribution $g(\boldsymbol{z})$, where $\boldsymbol{z} = (\boldsymbol{R}, v_\parallel, \mu)$ is 5D phase space coordinates

$$g(z,t) \approx \sum_{p=1}^{N} \frac{\delta[z_p - z_p(t)]}{J_z}$$

The physical distribution $f(\boldsymbol{z}, t)$ is represented as

$$f(z,t) = P_{tot}(z,t)g(z,t) \approx \sum_{p=1}^{N} p_{p,tot}(t)\frac{\delta[z_p - z_p(t)]}{J_z} \quad ,$$

where $P_{tot}(\boldsymbol{z}, t) = \frac{f(\boldsymbol{z},t)}{g(\boldsymbol{z},t)} = \frac{n_f}{\langle n_f \rangle_V} \frac{\langle n_g \rangle_V}{n_g} \frac{f_v}{g_v}$

[Z Lu, G Meng, R Hatzky, M Hoelzl, P Lauber, PPCF(2023)] & refs. Therein; also in PICLS, Boesl, Bottino et al

δf scheme: summarized in ORB5 work [Lanti19]

With decomposition $f = f_0 + \delta f$

$$f_0(z,t) = P(z,t)g(z,t) \approx \sum_{p=1}^{N} p_p(t)\frac{\delta[z_p - z_p(t)]}{J_z}$$

$$\delta f(z,t) = W(z,t)g(z,t) \approx \sum_{p=1}^{N} w_p(t)\frac{\delta[z_p - z_p(t)]}{J_z}$$

where $P(\boldsymbol{z}, t) = \frac{f_0(\boldsymbol{z},t)}{g(\boldsymbol{z},t)}$,$W = \frac{\delta f(\boldsymbol{z},t)}{g(\boldsymbol{z},t)}$

Weight equations

$$\frac{d}{dt}w_p(t) = -p_i(t)\frac{d}{dt}\ln f_0(z_p(t)) \quad ,$$

$$\frac{d}{dt}p_p(t) = p_i(t)\frac{d}{dt}\ln f_0(z_p(t)) \quad .$$

[Lanti et al. *Computer Physics Communications*, 251, 107072 (2019)]

Mixed variable/pullback scheme for full f and δf models

Different expressions of mixed variables/pullback scheme for full f and δf

- **Goal:** $\nabla_\perp^2 \delta A_\parallel^{\mathrm{h}} - \sum_s \frac{1}{d_e^2} \overline{\langle \delta A_\parallel^h \rangle} = -\nabla_\perp^2 \delta A_\parallel^{\mathrm{s}} - \mu_0 \delta j_\parallel$

The parallel Ampere's law is solved iteratively

$$\left(\nabla_\perp^2 - \sum_s \frac{1}{d_s^2} \right) \delta A_{\parallel,0}^{\mathrm{h}} = -\nabla_\perp^2 \delta A_\parallel^{\mathrm{s}} - \mu_0 \delta j_{\parallel,u}$$

$$\left(\nabla_\perp^2 - \sum_s \frac{1}{d_s^2} \right) \delta A_{\parallel,p}^{\mathrm{h}} = -\sum_s \frac{1}{d_e^2} \delta A_{\parallel,\boldsymbol{p-1}}^{\mathbf{h}} + \sum_s \frac{1}{d_e^2} \overline{\langle \delta A_{\parallel,p-1}^h \rangle}$$

for δf model: $\overline{\langle \delta A_{\parallel,p-1}^h \rangle} = \frac{2}{n_0 v_{ts}^2} \int dz^6 v_\parallel^2 \langle \delta A_{\parallel,p-1}^h \rangle \delta(\boldsymbol{R} + \boldsymbol{\rho} - \boldsymbol{x}) f_0,$

for full f model: $\overline{\langle \delta A_{\parallel,p-1}^h \rangle} = \frac{1}{n_0} \int dz^6 \langle \delta A_{\parallel,p-1}^h \rangle \delta(\boldsymbol{R} + \boldsymbol{\rho} - \boldsymbol{x}) f,$

Ref.: derivation of sympletic/adiabatic current in Hatzky19

Key idea: noise cancels noise

Rigorously speaking, this correction is crucial; $\frac{-1}{n_0} \int dz^6 v_\parallel \frac{\partial \ln f_0}{\partial v_\parallel} \ldots \neq \frac{1}{n_0} \int dz^6 \langle \delta A_{\parallel,p-1}^h \rangle f \ldots$

TRIMEG-GKX: demo (simplified) code with circular geometry
TRIMEG-C1: mixed spline-unstructured mesh for realistic geometry

- **Software engineering: MVP (minimum viable prototype) → bigger code**
- **Analytical ad-hoc equilibrium, spline in 3 directions, full f & δf, mixed variable & pullback**
- **Structures: particle and field on the same level**
- **TRIMEG-GKX: ~6000 lines in Fortran; ~5000 lines in Matlab**
- **Similar structures except MPI, solver, visualization**

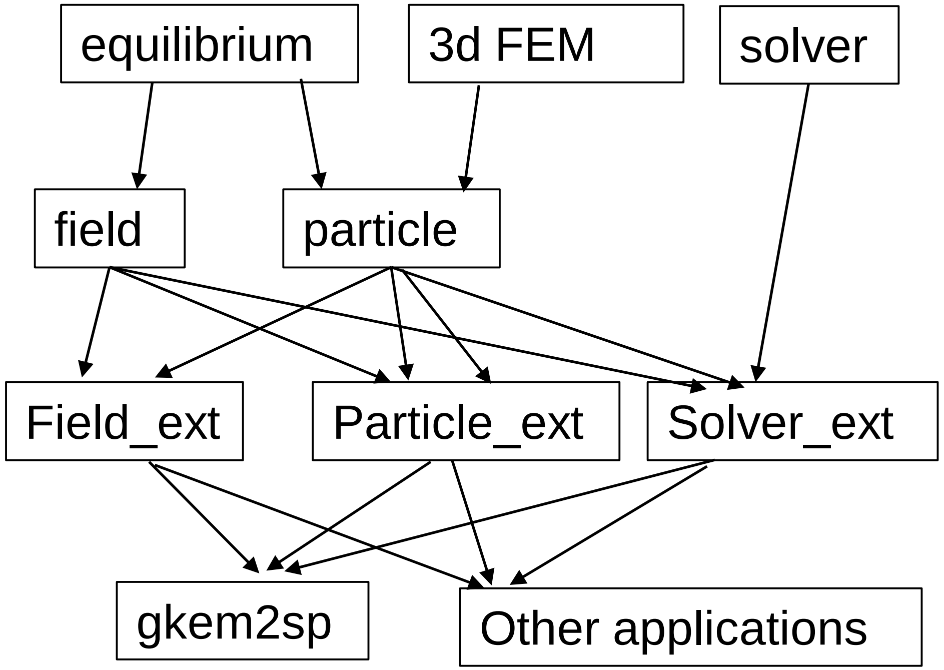

- **TRIMEG-C1: ~8000 lines (kernel) in Fortran**
- **Field solver: PETSC; w/ particle decomposition; w/o domain decomposition (shared memory for field)**

Results: TRIMEG-GKX (pure cubic spline; ad-hoc equilibrium)

Benchmark of ITPA-TAE case: reasonable agreement

The growth rate and the mode structure agree with previous results [Koenies18NF]

- δf scheme for all 3 species; realistic mass ratio ($\frac{m_i}{m_e} = 1836$)

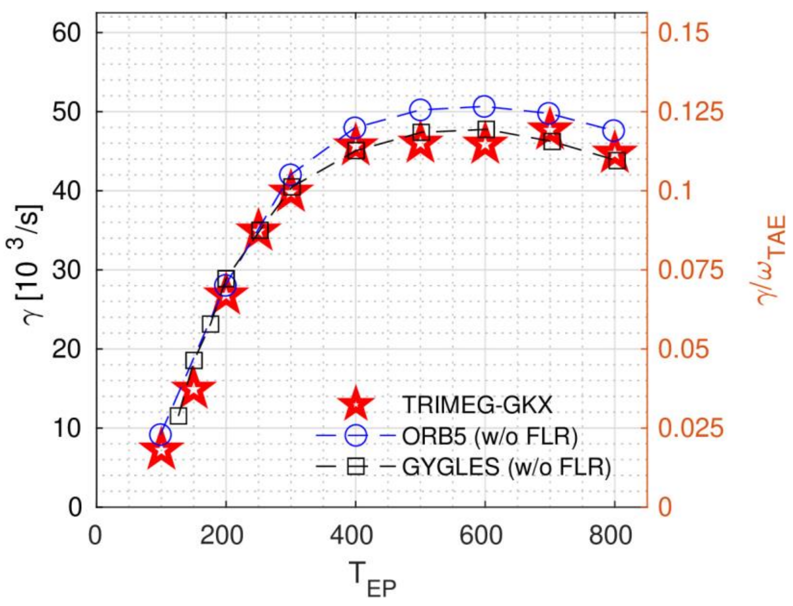

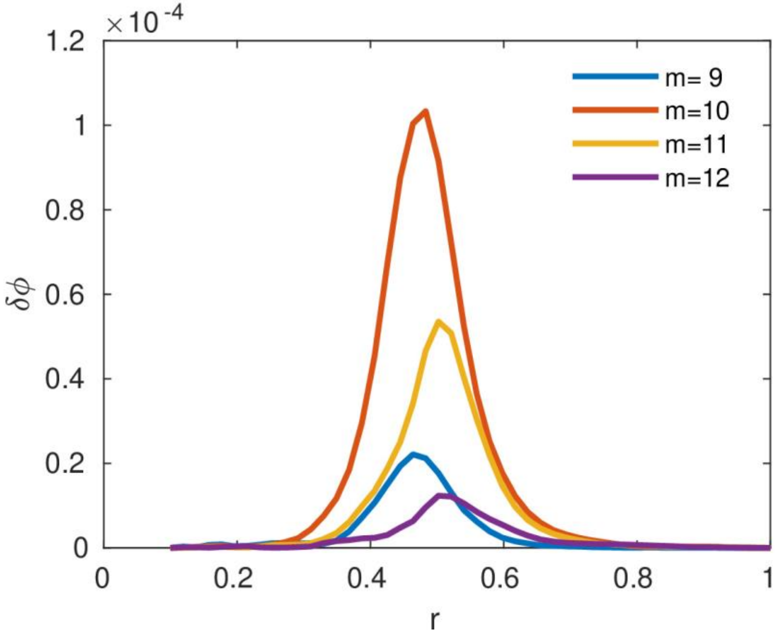

Mixed full f–δf simulations

Full f EPs, δf electrons & thermal ions: more efficient

Full f: growth rate ~40% lower than the δf results, if local Maxwellian distribution is used

EP gradient ($\frac{\mathrm{d}\ln n}{\mathrm{d}r}$) relaxes for $\sim 40\%$ for $T_{\mathrm{EP}} = 400\ \mathrm{keV}$

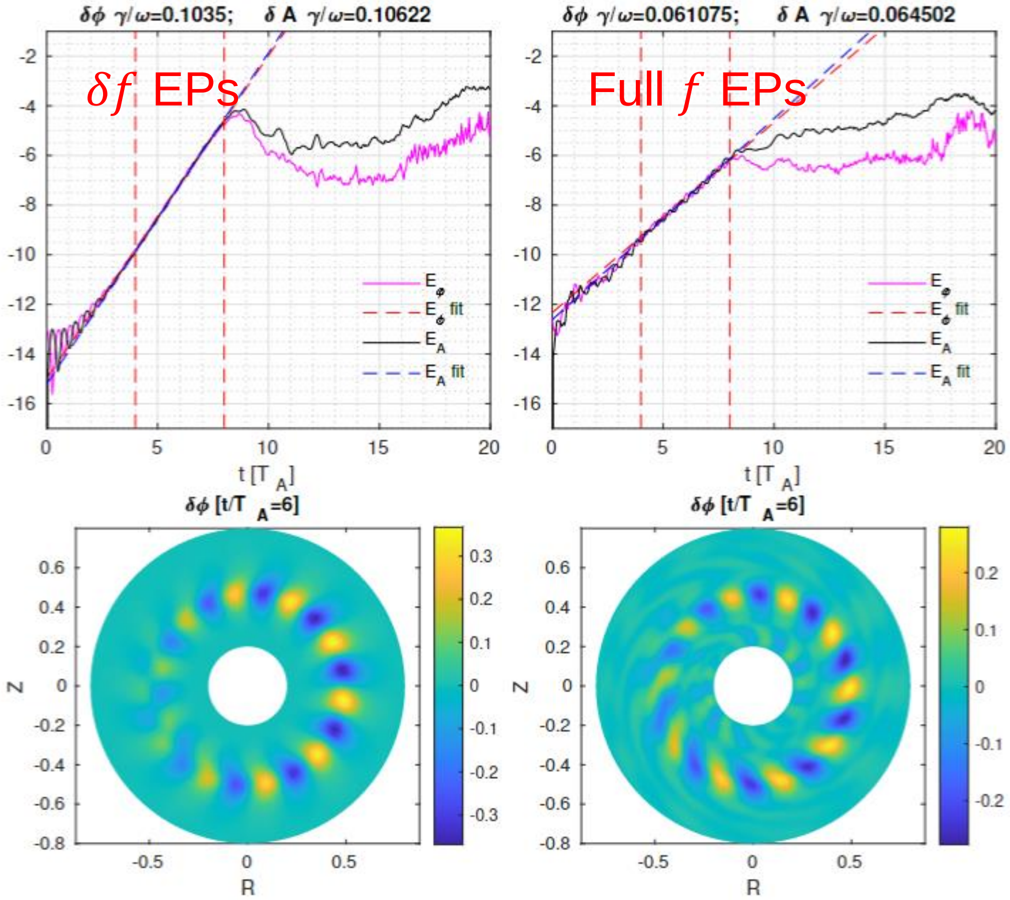

Full f EP simulations with constant of motion EP distribution

EP distribution in Constants of Motion (COM) space: $f(\psi_{cs}, E, \Lambda)$

- Shifted canonical toroidal momentum:

$$\psi_{cs} = \psi + \frac{mF}{qB} v_{\parallel} - sign(v_{\parallel})\sqrt{2(E-\mu B_0)}\frac{mF}{qB_0} H(E-\mu B_0)$$

- ψ_{cs} describes the radial location of orbit center

Local Maxwellian EP distribution is not a good approximation, especially when EP energy is high and for full f

- In δf simulations, the EP distribution can be forced to be Maxwellian analytically; but the marker distribution will deviate from its initial one if markers are not loaded in constants of motion space

Two ways of starting full f simulations from stationary distributions

- Scheme 1: Load markers in constant of motion space, uniformly distributed along the ignorable angle

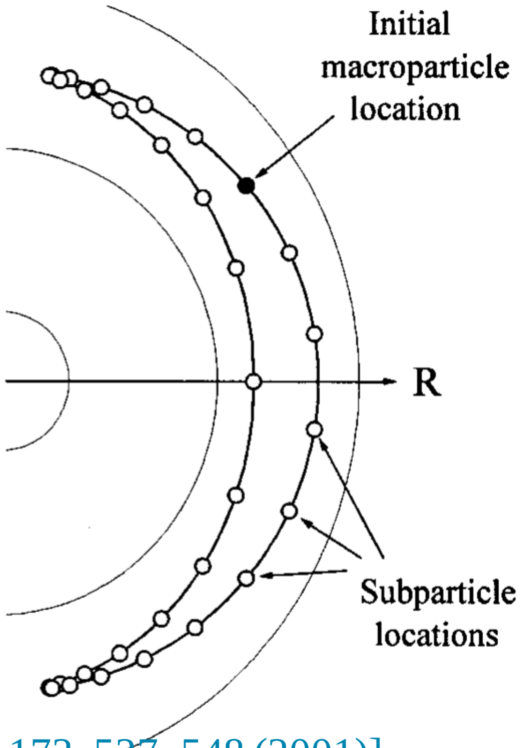

[Heikkinen et al, JCP 173, 527–548 (2001)]
[Bierwage et al, CPC 183 (2012) 1107; CPC 275, 108305 (2022)]

- Scheme 2: Load markers with a chosen distribution, modify f/g (f, g: particle or marker distribution), so that the physical distribution is stationary in constant of motion space (this work)
- $f = \frac{N}{N_p} \sum_p \frac{w_{p,tot}}{J} \delta(\boldsymbol{R} - \boldsymbol{R_p}) \delta(\boldsymbol{v}_\parallel - \boldsymbol{v}_{\parallel \boldsymbol{p}}) \boldsymbol{\delta}(\boldsymbol{\mu} - \boldsymbol{\mu_p})$
- $w_{p,tot} = f/g$; J: Jacobian
- $g(r, \theta, v) = \frac{N_p}{\pi^{3/2} v_{th}^3 V_{tot}} \frac{R_0}{R} e^{-\frac{mv^2}{2T}}$; uniform along R, Z, ϕ
- $f = f(\psi_{cs}, v) = \frac{n(\psi_{cs})}{\pi^{3/2} v_{th}^3} e^{-\frac{mv^2}{2T}}$
- Thus $w_{p,tot} = \frac{n(\psi_{cs}) V_{tot} R}{N_p R_0}$

[Lu et al JCP2021, PPCF2023, same philosophy as Hatzky2019]

Marker loading using local Maxwellian versus constants of motion

- For simulations starting from local Maxwellian EP distribution, a relaxation in density profile occurs in few transit periods ($t/T_A \sim 1$). Density gradient & growth underestimated by $\sim 40\%$
- Using constants of motion, markers are loaded to represent the stationary EP distribution

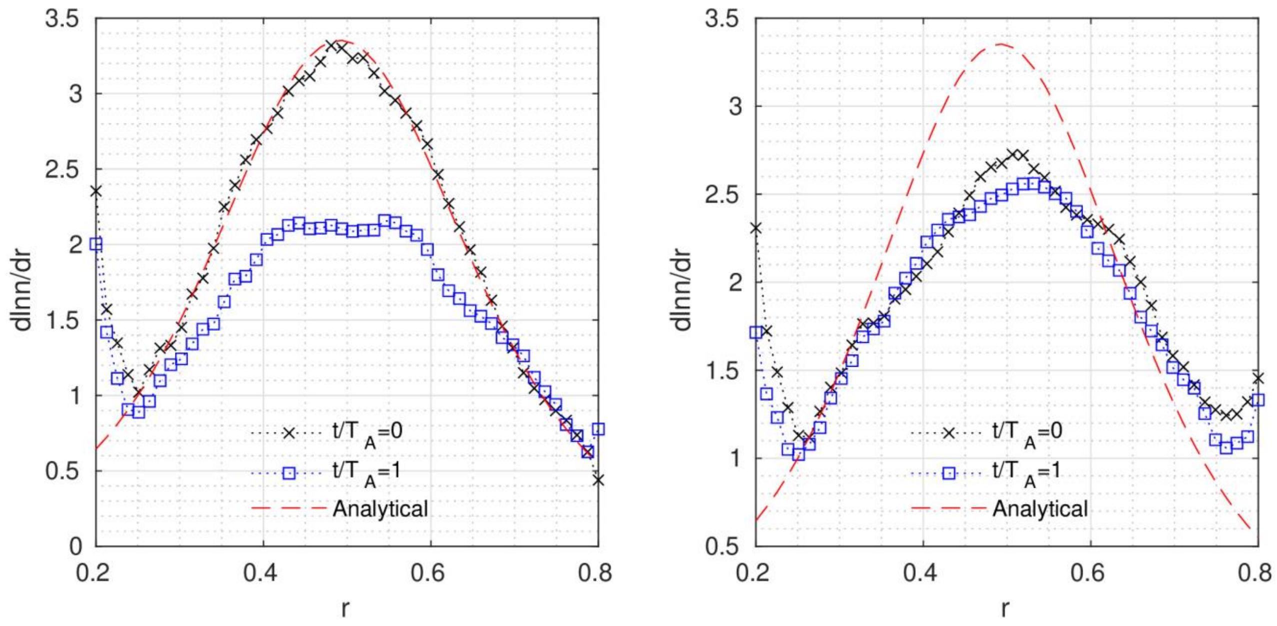

- Red dashed line: target density gradient profile
- Left: load markers with $f_{loc} = n(r)\exp\left\{-\frac{mE}{T}\right\}$
- Right: load markers with $f_{COM} = n(r_{cs})\exp\{-\frac{mE}{T}\}$

$$r_{cs}^2 = \frac{\psi_{cs}-\psi_{axis}}{\psi_{edge}-\psi_{axis}};$$

$$\psi_{cs} = \psi + \frac{mF}{qB} v_\parallel - sign(v_\parallel)\sqrt{2(E-\mu B_0)}\frac{mF}{qB_0} H(E-\mu B_0)$$

- $n(r) = n_0 c_3 \exp\left\{-\frac{c_2}{c_1}\tanh\frac{r-c_0}{c_2}\right\}$

Full f simulations matched to δf simulations

- **Distribution in constant of motion mitigates artificial density relaxation**
- **But $n(r_{cs})$ specifies the orbit density; $n(r)$: particle density**
- **Match between $n(r_{cs})$ and $n(r)$: mapping between the distribution in (shifted) orbit center and that in particle location**
- **EP relaxation is avoided; EP profile and growth rate matched to δf results**

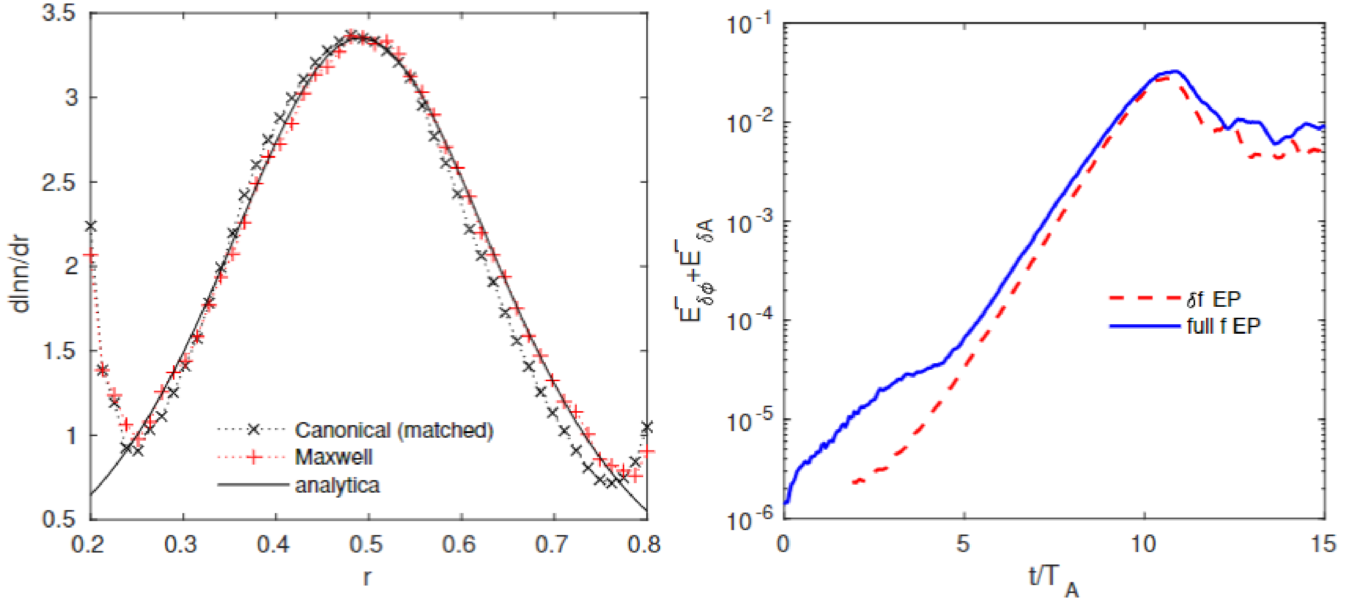

[Z Lu, G Meng, R Hatzky, M Hoelzl, P Lauber, PPCF (2023)]

TAE simulations (moderate d_e) in TRIMEG-C1

- **Unstructured meshes are generated for circular geometry**
- **TAE oscillation simulated using the modified ITPA-TAE parameters**
  - $n = 2, \beta = \frac{10^{-4}}{9}, \frac{m_e}{m_p} = \frac{1}{200}$
  - **nominal:** $n = 6, \beta = 9 \times 10^{-4}, \frac{m_e}{m_p} = \frac{1}{1836}$
- **Magnetic axis is included**
- **Two species; pure $p_\parallel$ form**
- **18 radial grids, 8 grids/per toroidal wave length**
- **Ongoing: simulations with smaller electron skin depth (d_e), longer time scale, higher resolution.**

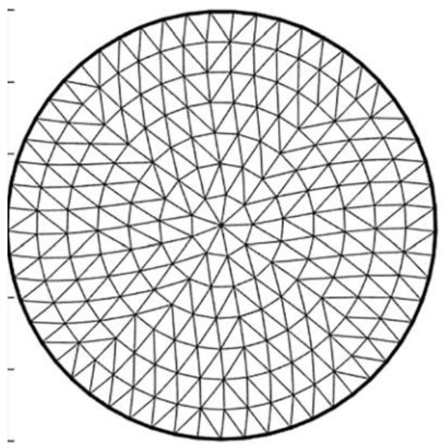

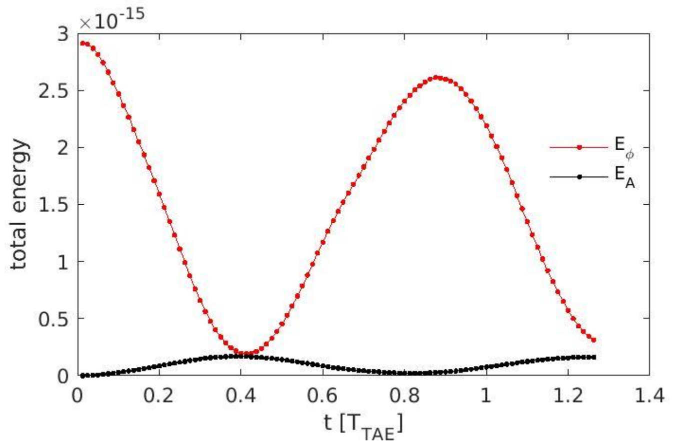

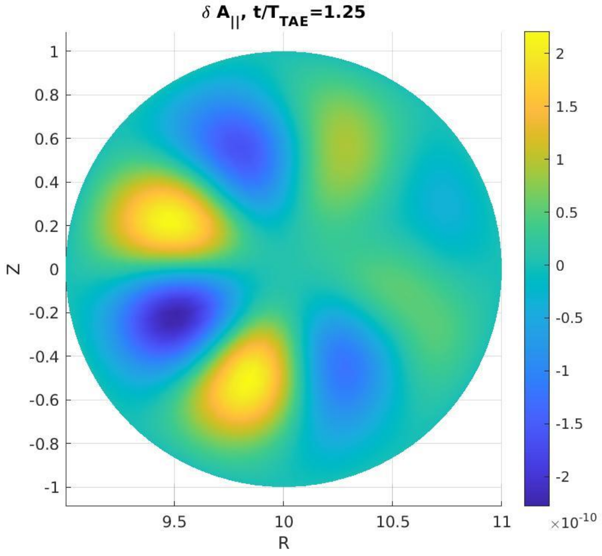

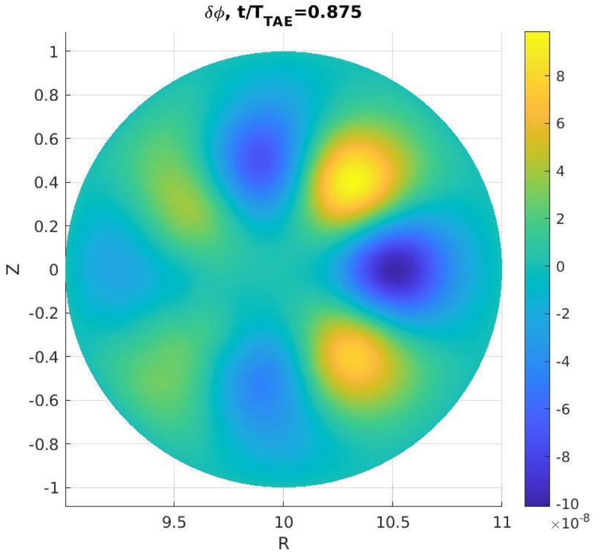

Other ongoing studies

Neoclassical physics

Full f nonlinear collision operator

Field-aligned finite element method

A) Neoclassical physics in TRIMEG-C0

The Lorentz collision model w/o E_r solver is implemented in TRIMEG-C0: electron transport and bootstrap current (Lana Rekhviashvili; master thesis)

δf scheme; Bootstrap current, electron particle/energy fluxes agree with theory (R/a=10)

High/low collisionality (upper/bottom): good agreement with local theory

Particle simulations is capable in larger parameter regimes (large orbit width, global effects etc) than local theory

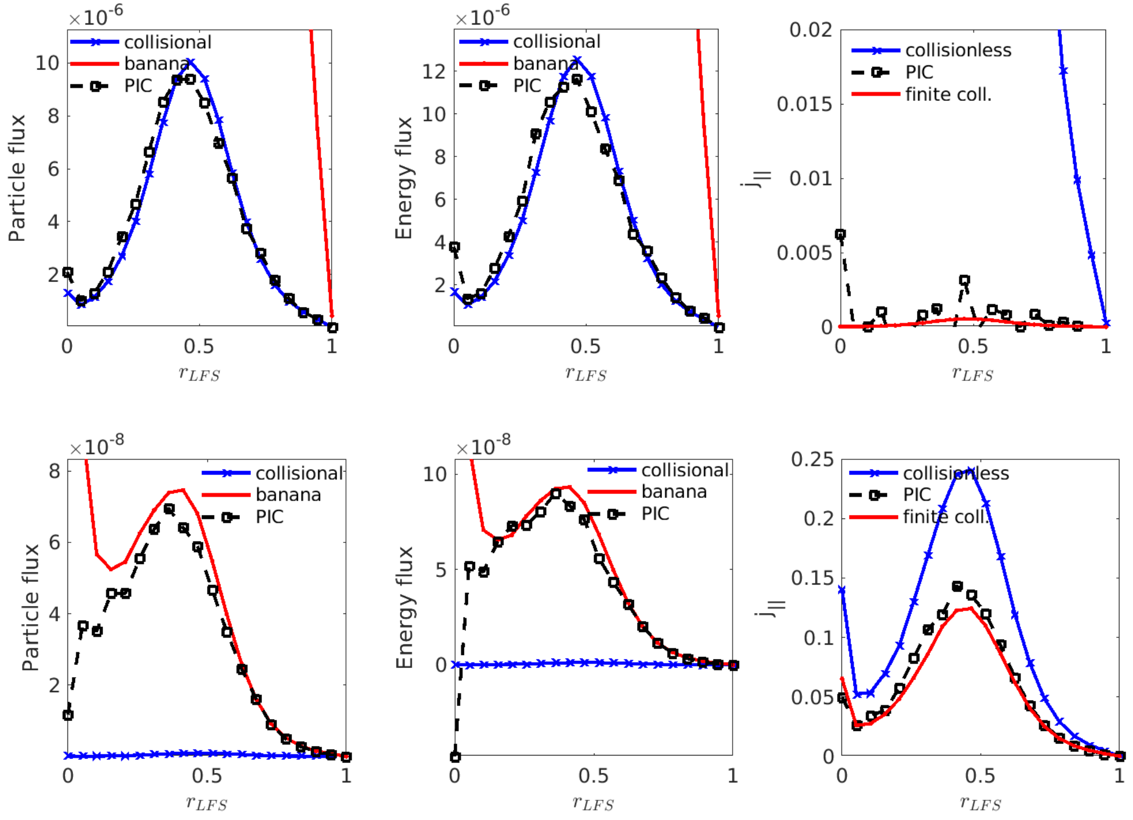

[L. Rekhviashvili, master thesis; arXiv preprint arXiv:2303.00415]

Neoclassical physics with E_r in TRIMEG-GKX

Parallel line in TRIMEG-GKX: multi-species model, with Lorentz collision & E_r solver

- Flat T case (only n variation)

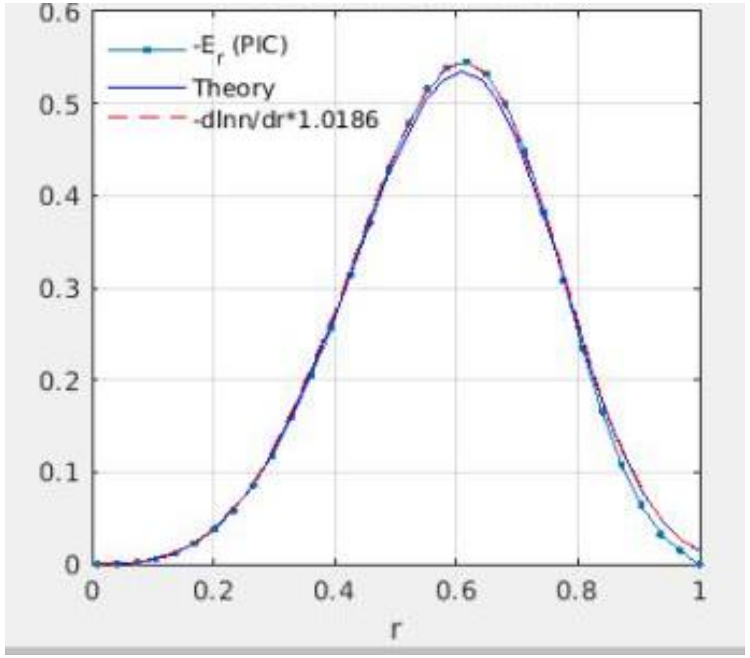

B) Full f nonlinear collision operator: aims for reducing cost from N_p^2 to αN_p in 0d2v/3v, large marker # limit

Fully nonlinear collision operator (species a scattered by b):

$$\frac{1}{\Gamma}\frac{\partial f_a}{\partial t} = -\frac{m_a+m_b}{m_b}\frac{\partial}{\partial \boldsymbol{v}}\cdot\left[f_a\frac{\partial}{\partial \boldsymbol{v}}h(\boldsymbol{v})\right] + \frac{1}{2}\frac{\partial}{\partial \boldsymbol{v}}\cdot\frac{\partial}{\partial \boldsymbol{v}}\cdot\left[f_a\frac{\partial}{\partial \boldsymbol{v}}\frac{\partial}{\partial \boldsymbol{v}}g(\boldsymbol{v})\right] \quad (1)$$

Integral form: $h(\boldsymbol{v}) = \int d\boldsymbol{v}\frac{f_b(\boldsymbol{v}')}{|\boldsymbol{v}-\boldsymbol{v}'|}$, $g(\boldsymbol{v}) = \int d\boldsymbol{v} f_b(\boldsymbol{v}')|\boldsymbol{v}-\boldsymbol{v}'|$ (2)

Elliptic equation: $\frac{\partial}{\partial \boldsymbol{v}}\cdot\frac{\partial}{\partial \boldsymbol{v}}h(\boldsymbol{v}) = -4\pi f(\boldsymbol{v})$, $\frac{\partial}{\partial \boldsymbol{v}}\cdot\frac{\partial}{\partial \boldsymbol{v}}g(\boldsymbol{v}) = 2h(\boldsymbol{v})$ (3)

- Valid for arbitrary distribution function; no expansion near Maxwellian
- 0d2v/3v, Directly solving (2): $N_p \times N_g$, N_p: particle #, N_g: $\boldsymbol{v}$ grid number
- Solving (3): field Degree of Freedom is N_g; particle-to-field projection: $O(1)N_p$
- Upper limit of cost: $N_p \times N_g$ or $O(\ll N_g)N_g + O(1)N_p$
- Mixed direct-elliptic solver is developed, in test code
- Pros: lower consumption (than 2 body-collisions $\sim \boldsymbol{N_p^2}$); Cons: rigorous conservation is not obvious
- Possible improvement: control variate scheme [Sonnendrücker, et al. *JCP* 295, 402 (2015)]; or improvement in solving Langevin equation (w/ inputs from C. Slaby, R. Kleiber)

w/ input from A. Chankin, A. Bergmann, G. Meng et. al.

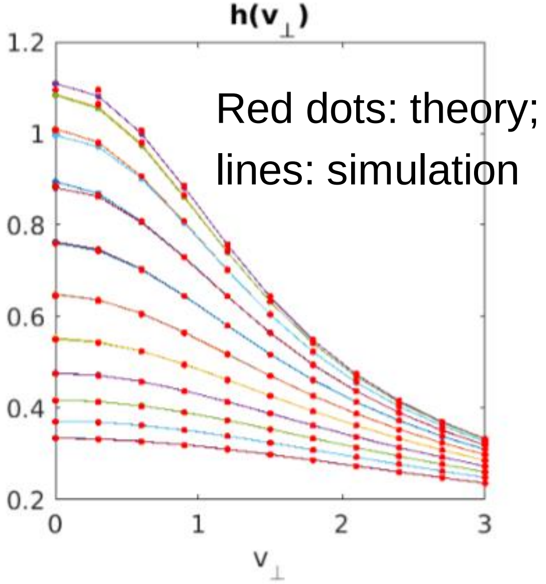

Numerical/physics tests of nonlinear collision operators

Maxwellian distribution as a steady state

- **Deviation from Maxwellian appears if time step size is large**

Time evolution of a bump-on-tail distribution

- **Relaxation from bump-on-tail to Maxwellian is simulated**
- **Conservation improves as time step size decreases**

2d2v model ongoing (full f neoclassical physics)

Key issue: how to get better/rigorous conservation?

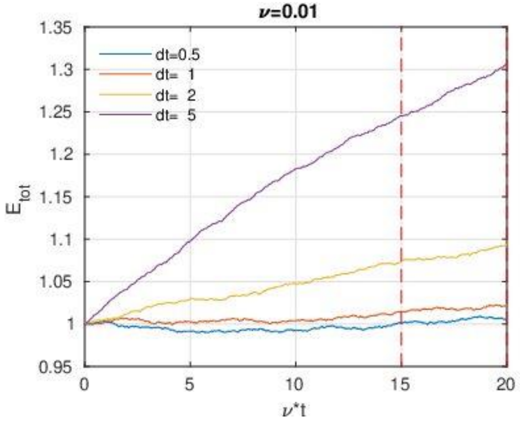

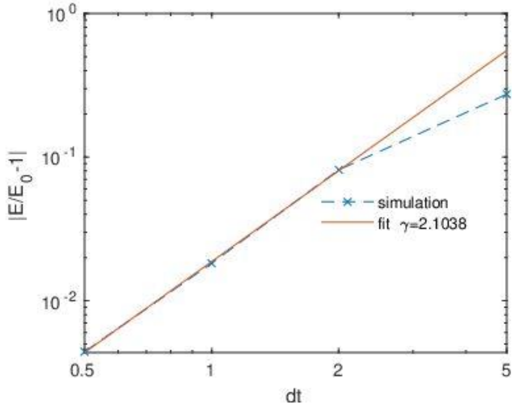

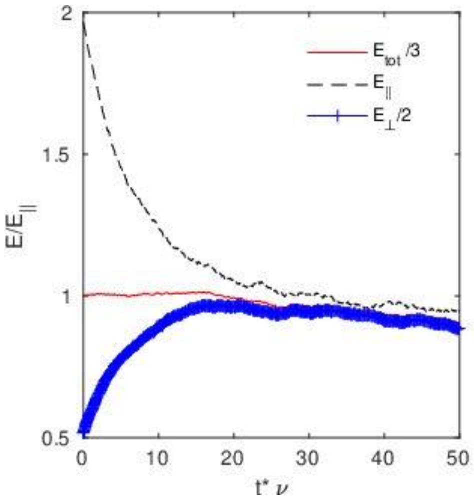

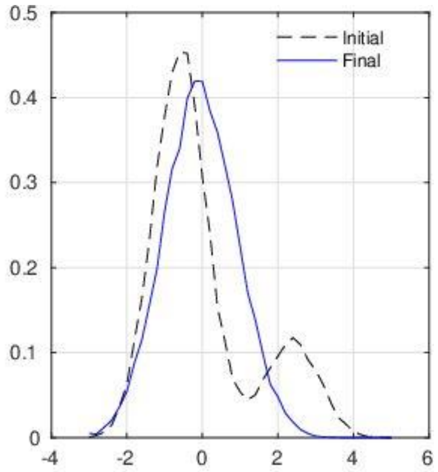

C) Field-aligned finite element: for multi-(high) n NL simulations

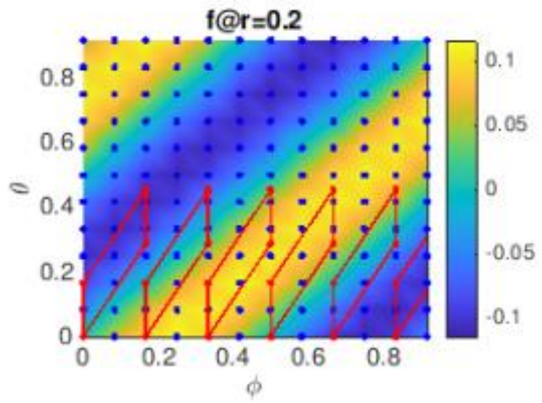

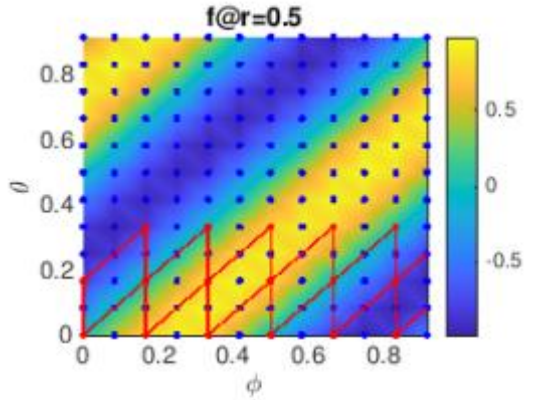

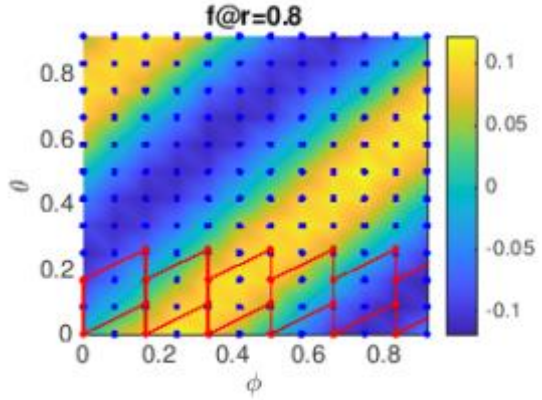

- All grids are aligned without shift
- Basis functions are defined on piecewise field-aligned coordinate
- The grid number in the parallel direction can be reduced greatly
- Convergence relies on marker #, grid # in 3 directions, order of finite element basis functions
- Linear/cubic finite element implemented (3d Vlasov-Poisson problem, δf scheme); goal: $n_\phi = 16$ or $32; n_\theta = 512; n_r = 64$ for $\boldsymbol{n} \in \mathbf{0}, \mathbf{1}, \dots, \mathbf{128}]$

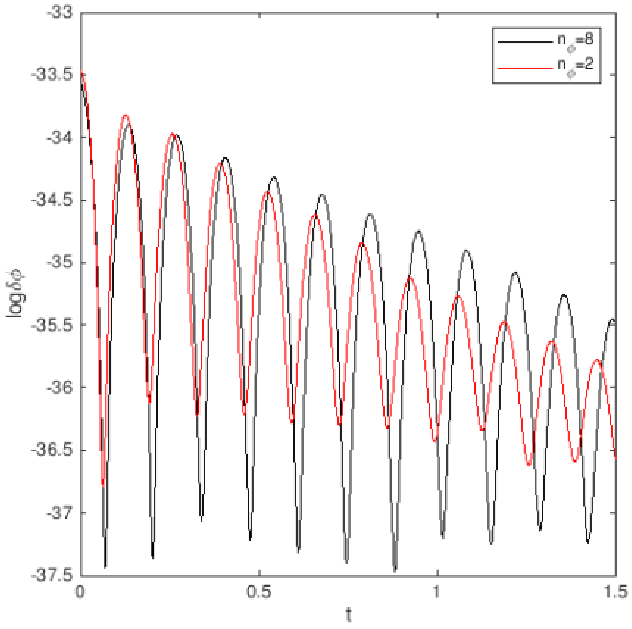

Grid # $n_\phi = 2$

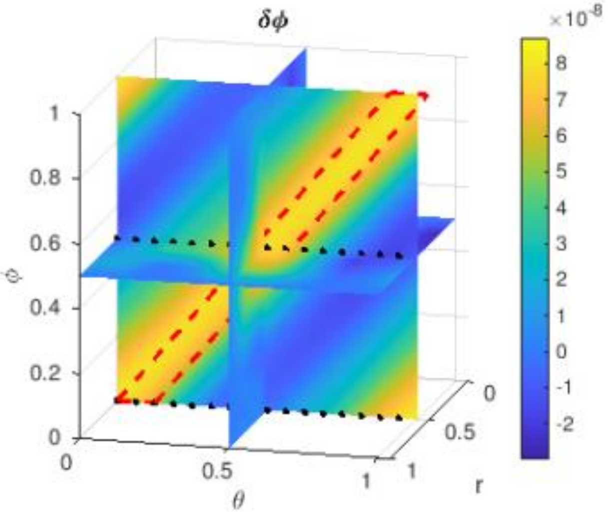

Grid # $n_\phi = 8$

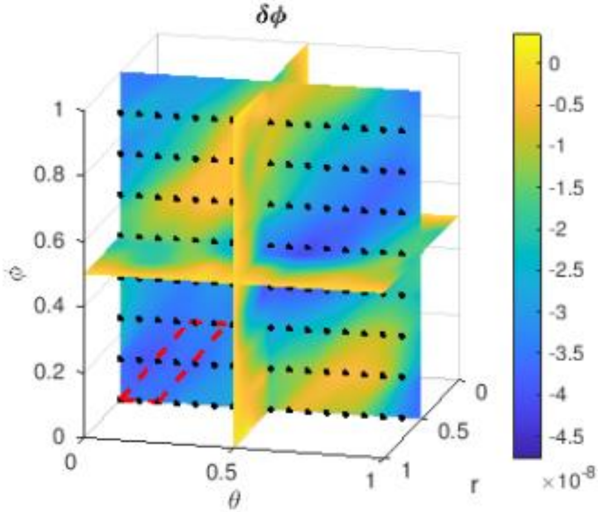

Construction in tokamak geometry

- **The Clebsch coordinate is calculated numerically $\eta = \eta(r, \theta, \phi)$, $r = \sqrt{(\psi - \psi_{axis})/(\psi_{edge} - \psi_{axis})}$**
- **Equations are represented in the Clebsch coordinates (r, η, ϕ)**
- **Partition of unit is satisfied (issue raised by Eric)**
- **Strong deformation of poloidal grids avoided; periodicity along θ and ϕ are satisfied (issue raised by Laurent, Matthias et al)**

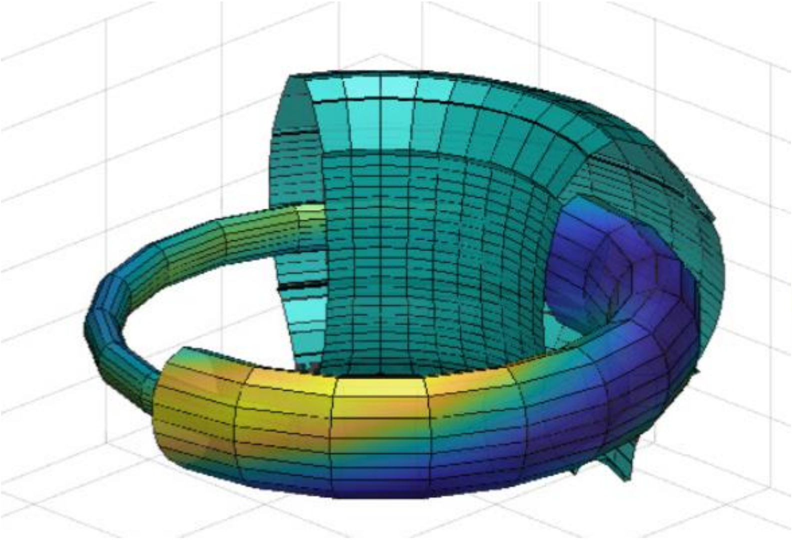

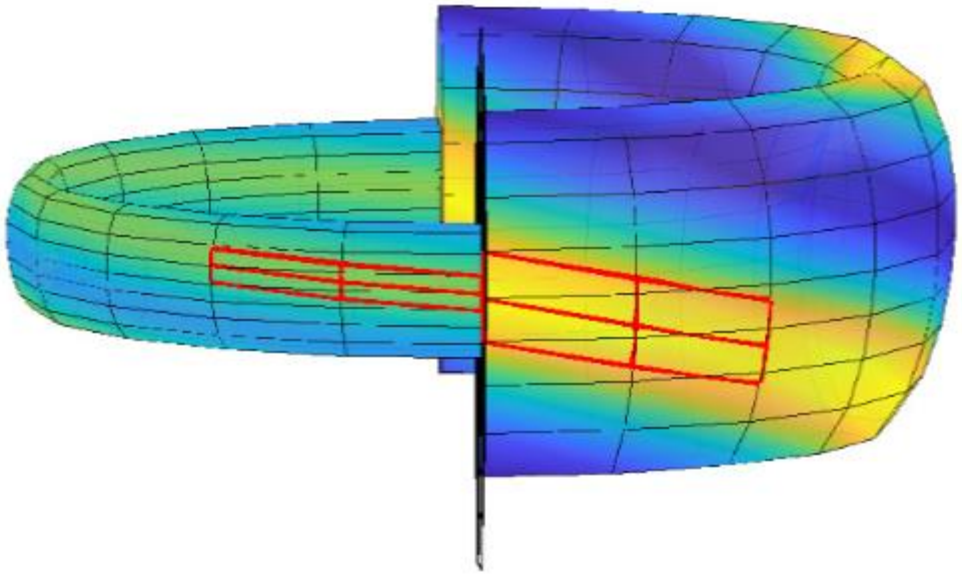

- Grid deformation for large/small toroidal grids # $\eta(r, \theta, \phi)$

@ϕ_8

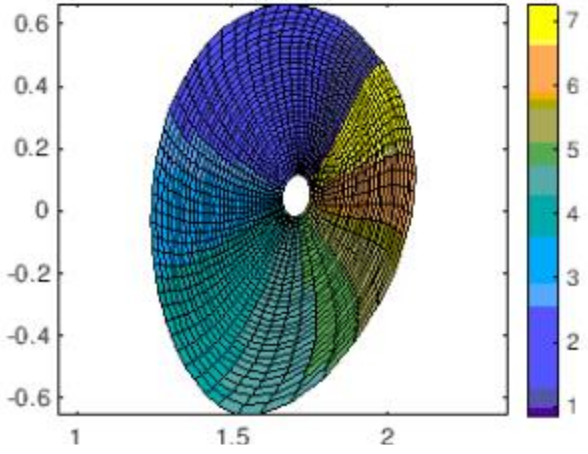

@ϕ_5

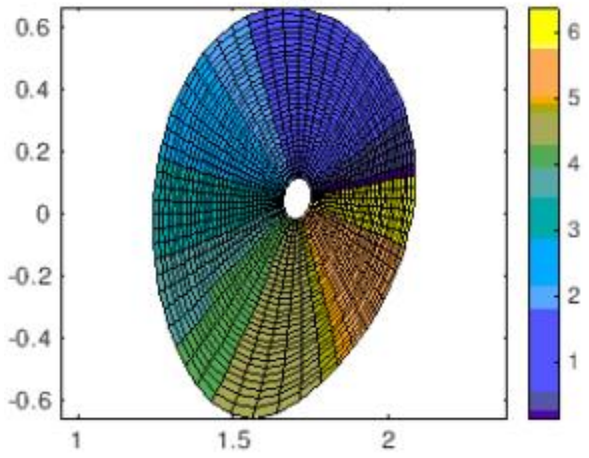

Conclusions and outlook

Summary

- EP driven TAE simulated for small electron skin depth limit ($d_e \sim 10^{-3}$) with MV/PB scheme
- The mixed full f-δf scheme has been implemented for EP driven TAEs
- The EP simulations using constant of motion is especially useful in full f schemes

- ITG/TEM with kinetic electrons/EM effects are simulated in TRIMEG-C1

Outlook

- Aiming for physics studies with X point, EM and kinetic electrons
- Field aligned coordinate in parallel direction, unstructured mesh in (R, Z): merit more effort
- Application to EP/AE studies in AUG experiments merits more effort
- Implementation of the EM GK model in JOREK can lead to a powerful tool
- Full f collision might reveal interesting physics (NC-instability synergy, edge coupling etc.)

Backup slides

TRIMEG-C1

Implicit full-f scheme using $v_\parallel$ form

- Particle enslavement makes it possible
  - Degree of freedom reduced to field grid size

[G. Chen & Chacon 230(18), 2011 J. Comp. Phys.]

- Moment enslavement is proposed by us
  - Starting from particle enslavement
  - Achieved: good convergence of the implicit particle-field system
  - TAE w/o and with EPs are simulated; good agreement with LIGKA for the ITPA-TAE case

[Z.X. Lu, G. Meng, M. Hoelzl, Ph. Lauber, Journal Comput. Phys. 440 (2021) 110384]

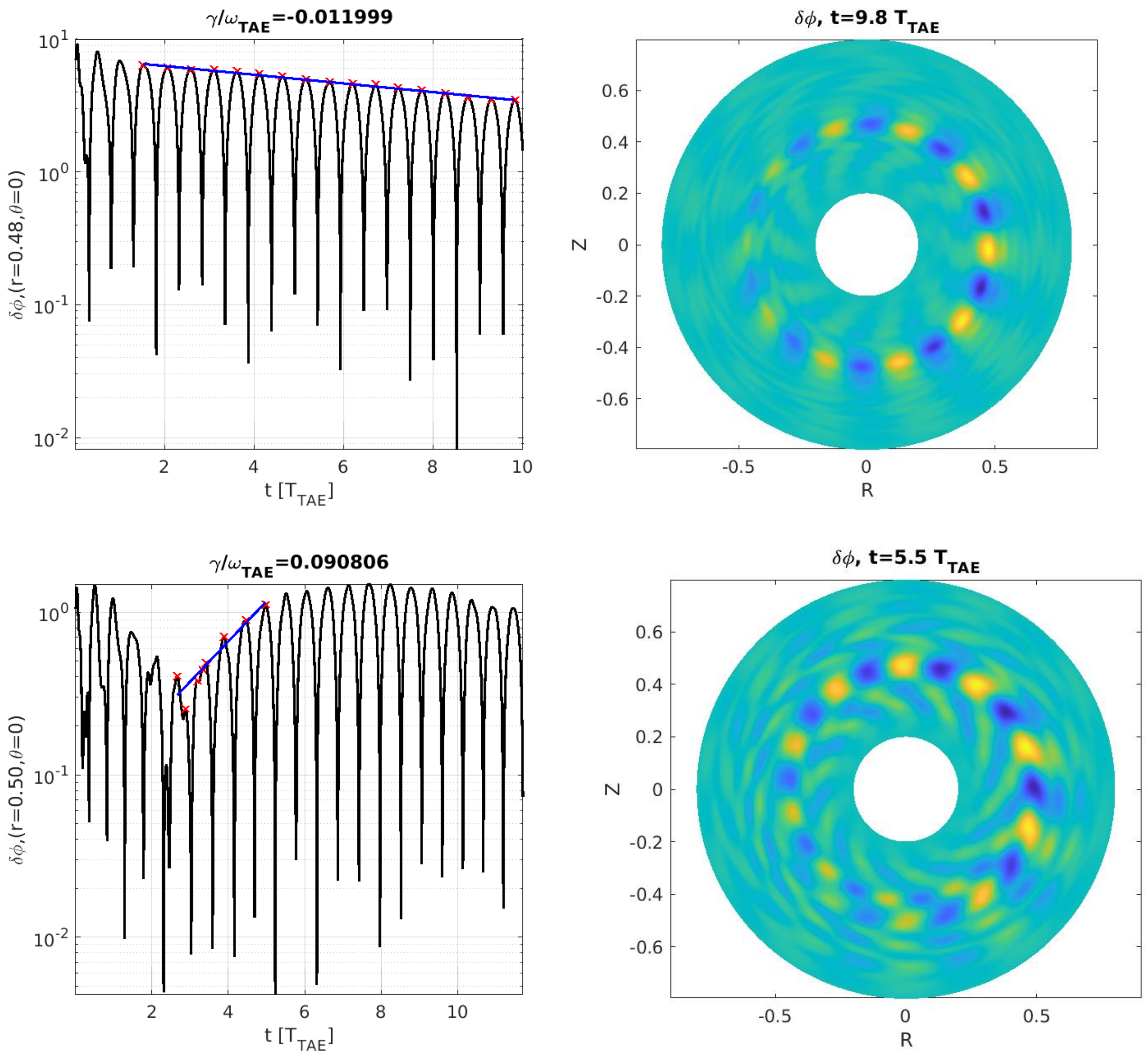

Good convergence achieved in particle-field implicit solver

In order to get good convergence of the implicit field-particle solver, the relative correction in $\delta\phi$ and $\delta A_\parallel$ in every iteration are analyzed [Z.X. Lu, G. Meng, M. Hoelzl, Ph. Lauber, Journal Comput. Phys. 440 (2021) 110384]

$$\xrightarrow{1}\begin{Bmatrix}\delta\Phi^{start}(t+\Delta t)\\ \delta A_\parallel^{start}(t+\Delta t)\end{Bmatrix}^i \xrightarrow{2}\begin{Bmatrix} l(t+\Delta t)\\ v_\parallel(t+\Delta t)\end{Bmatrix}^i \xrightarrow{3}\begin{Bmatrix}\delta N^{end}(t+\Delta t)\\ \delta J^{end}(t+\Delta t)\end{Bmatrix}^i \xrightarrow{3}\begin{Bmatrix}\delta\Phi^{end}(t+\Delta t)\\ \delta {A_\parallel}^{end}(t+\Delta t)\end{Bmatrix}^i \xrightarrow{4}\begin{Bmatrix}\delta\Phi^{start}(t+\Delta t)\\ \delta A_\parallel^{start}(t+\Delta t)\end{Bmatrix}^{i+1}$$

- **In Step 4: set field for the next iteration, $\{\delta\phi^{start}, \delta A_\parallel^{start}\}^{i+2} = \{\delta\phi^{end}, \delta A_\parallel^{end}\}^{i+1} + \{\Delta\delta\phi, \Delta\delta A_\parallel\}$; where $\{\Delta\delta\phi, \Delta\delta A_\parallel\}$ is solved from additional equations (moment enslavement)**

- Good convergence achieved (left: XGC; right: Lu2021)

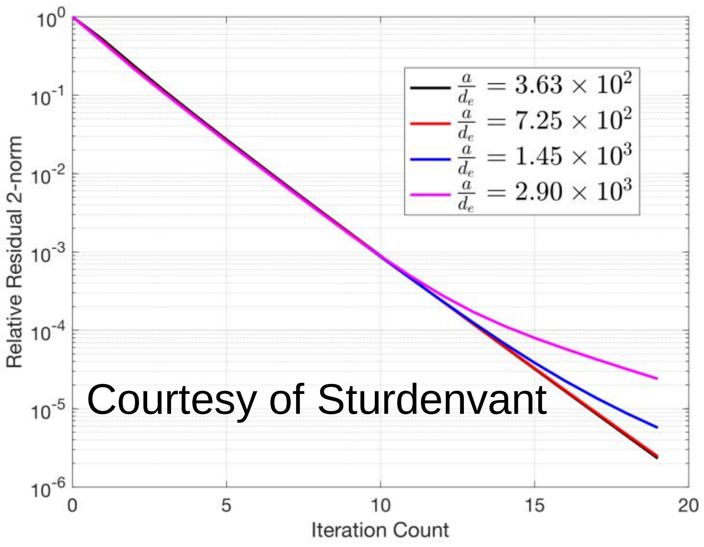

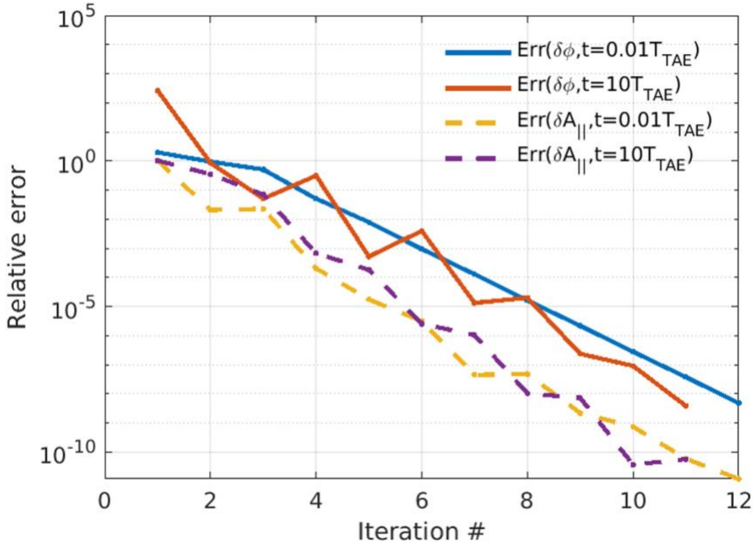

Guiding center's equations of motion

Using mixed variables, GC equations of motion are as follows

- $\frac{d\boldsymbol{R}_0}{dt}, \frac{du_{\parallel,0}}{dt}$: velocity, acceleration in magnetic equilibrium
- $\frac{d\delta\boldsymbol{R}}{dt}, \frac{d\delta u_{\parallel}}{dt}$: velocity, acceleration due to perturbed field

$$\frac{\mathrm{d}\mathbf{R_0}}{\mathrm{d}t} = v_{\|}\mathbf{b}^* + \frac{m\mu}{qB^*}\mathbf{b}\times\nabla B \ ,$$

$$\frac{\mathrm{d}u_{\|,0}}{\mathrm{d}t} = -\mu\mathbf{b}^*\cdot\nabla B \ ,$$

$$\frac{\mathrm{d}\delta\mathbf{R}}{\mathrm{d}t} = \frac{\mathbf{b}}{B^*}\times\nabla\langle\delta\phi - v_{\|}\delta A_{\|}\rangle \ ,$$

$$\frac{\mathrm{d}\delta u_{\|}}{\mathrm{d}t} = -\frac{q_s}{m_s}\left(\mathbf{b}^*\cdot\nabla\langle\delta\phi - v_{\|}\delta A_{\|}^{\mathrm{h}}\rangle + \partial_t\langle\delta A_{\|}^{\mathrm{s}}\rangle\right) - \frac{\mu}{B^*}\mathbf{b}\times\nabla B\cdot\nabla\langle\delta A_{\|}^{\mathrm{s}}\rangle \ ,$$

Ohm's law: $\partial_t\delta A_{\|}^{s} + \partial_{\|}\delta\phi = 0$

Some details of derivations of the symplectic current

$$u_\parallel = v_\parallel + \frac{q_s}{m_s}\delta A_\parallel^{\mathrm{h}}$$

Using mixed variables, denoting the physics (symplectic) current as $\boldsymbol{\delta j_{\parallel,v}}$

$$\nabla_\perp^2 \delta A_{\parallel,0}^{\mathrm{h}} = -\nabla_\perp^2 \delta A_\parallel^{\mathrm{s}} - \mu_0 \delta j_{\parallel,v}$$

Ignore finite Larmor radius (as an example)

In $\boldsymbol{\delta f}$ scheme, $\delta j_{\parallel,v} = \int d\boldsymbol{v} v_\parallel \delta f_v(v_\parallel) \approx \int d\boldsymbol{v}\left(u_\parallel - \frac{q_s}{m_s}\delta A_\parallel^{\mathrm{h}}\right)\left[\delta f_u(u_\parallel) + \frac{q_s}{m_s}\delta A_\parallel^{\mathrm{h}}\frac{\partial f_0}{\partial v_\parallel}\right]$

$$\approx \int d\boldsymbol{v} u_\parallel \left[\delta f_u(u_\parallel) + u_\parallel \frac{q_s}{m_s}\delta A_\parallel^{\mathrm{h}}\frac{\partial f_0}{\partial v_\parallel}\right] = \int d\boldsymbol{v} u_\parallel \delta f_u(u_\parallel) - \int d\boldsymbol{v}\frac{2u_\parallel v_\parallel}{v_{th}^2}\frac{q_s}{m_s}\delta A_\parallel^{\mathrm{h}}\frac{\partial f_0}{\partial v_\parallel}$$

In full $\boldsymbol{f}$ scheme, $\delta j_{\parallel,v} = \int d\boldsymbol{v} v_\parallel \delta f_v(v_\parallel) = \int d\boldsymbol{v}\left(u_\parallel - \frac{q_s}{m_s}\delta A_\parallel^{\mathrm{h}}\right) f_u$

$$= \int d\boldsymbol{v} u_\parallel f_u - \int d\boldsymbol{v}\frac{q_s}{m_s}\delta A_\parallel^{\mathrm{h}} f_u$$

Consistent with Hatzky19

where $f_u = f_u(u_\parallel - \frac{q_s}{m_s}\delta A_\parallel^{\mathrm{h}})$**; with Fourier filter, denoted as $\boldsymbol{\delta j_{\parallel,v}}$**

Convergence of the iterative Ampere solver

Good convergence of the iterative Ampere solver is observed

- $\left(\nabla_\perp^2 - \sum_s \frac{1}{d_s^2}\right)\delta A_{\parallel,p}^{\mathrm{h}} = -\sum_s \frac{1}{d_e^2}\delta A_{\parallel,\boldsymbol{p-1}}^{\mathbf{h}} + \sum_s \frac{1}{d_e^2}\overline{\langle \delta A_{\parallel,p-1}^{h}\rangle},$
  $\boldsymbol{p = 1, 2, 3 \ldots}$
- $\overline{\langle \delta A_{\parallel,p-1}^{h}\rangle}$ is calculated by the field-to-marker interpolation first, and then, the marker-to-field projection.

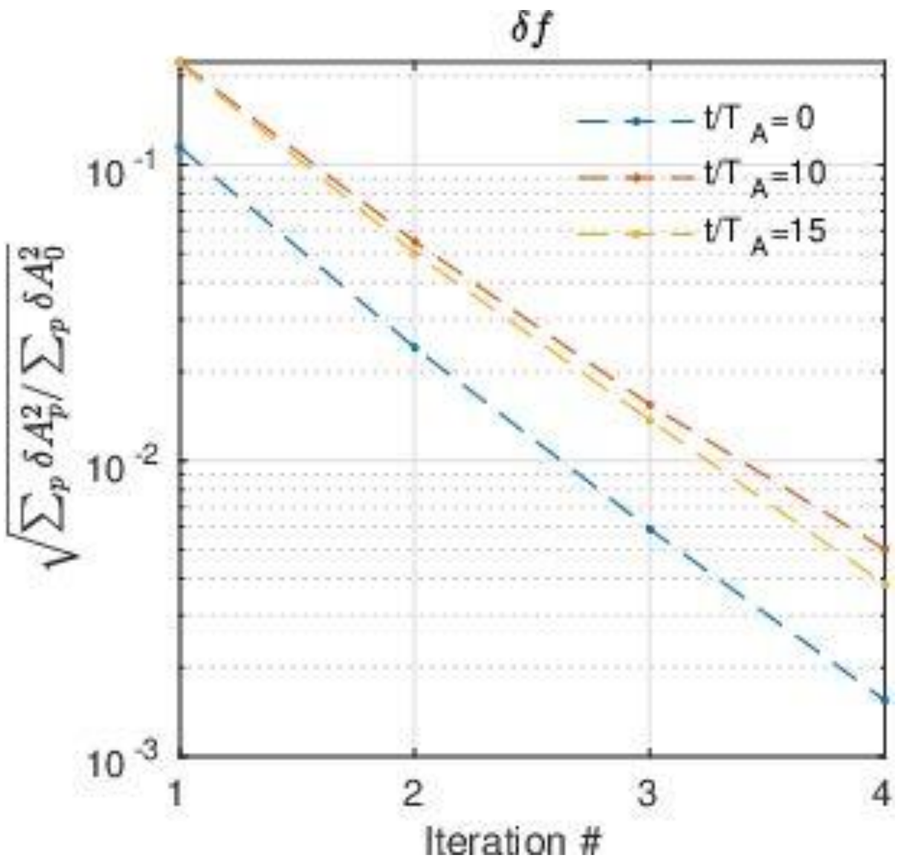

Convergence w.r.t. time step size and marker number

Good convergence observed as marker number > 10^6 and $\frac{\Delta t}{T_A} \leq 0.05$

40 steps /wave period already shows good accuracy

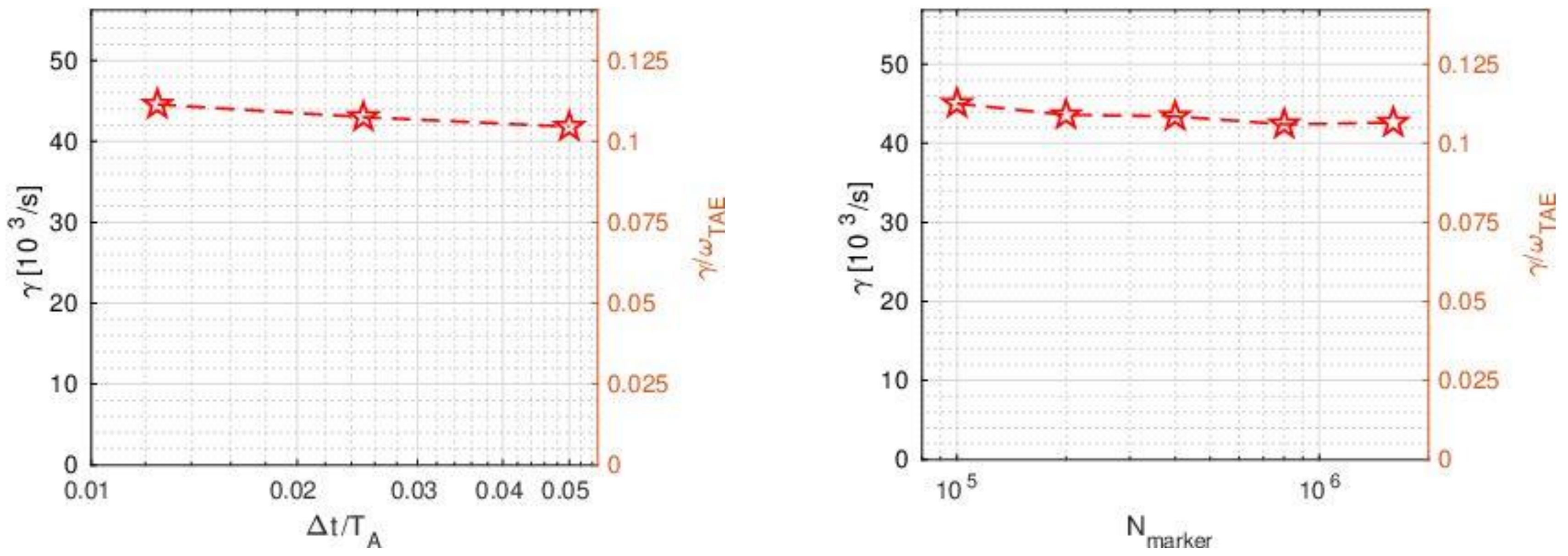

Results: TRIMEG-C1 (unstructured mesh; realistic geometry)

ongoing

C1 finite element: accuracy much better than C0

C1 Finite Element Method in triangular mesh shows good accuracy in field solver

- **C1 Error $\sim 1/N_r^5$ VS C0: $1/N_r^2$**
- 18 basis functions in each triangle
- $\nabla^2 sol = rhs$, solved in a rectangle

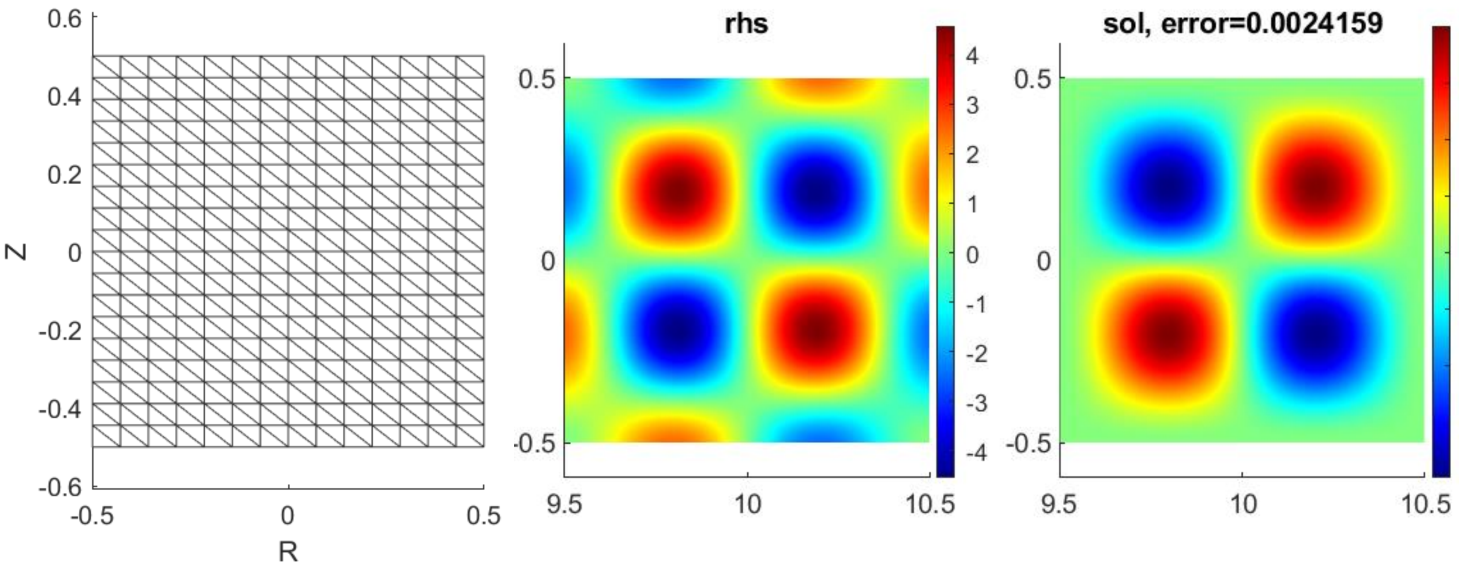

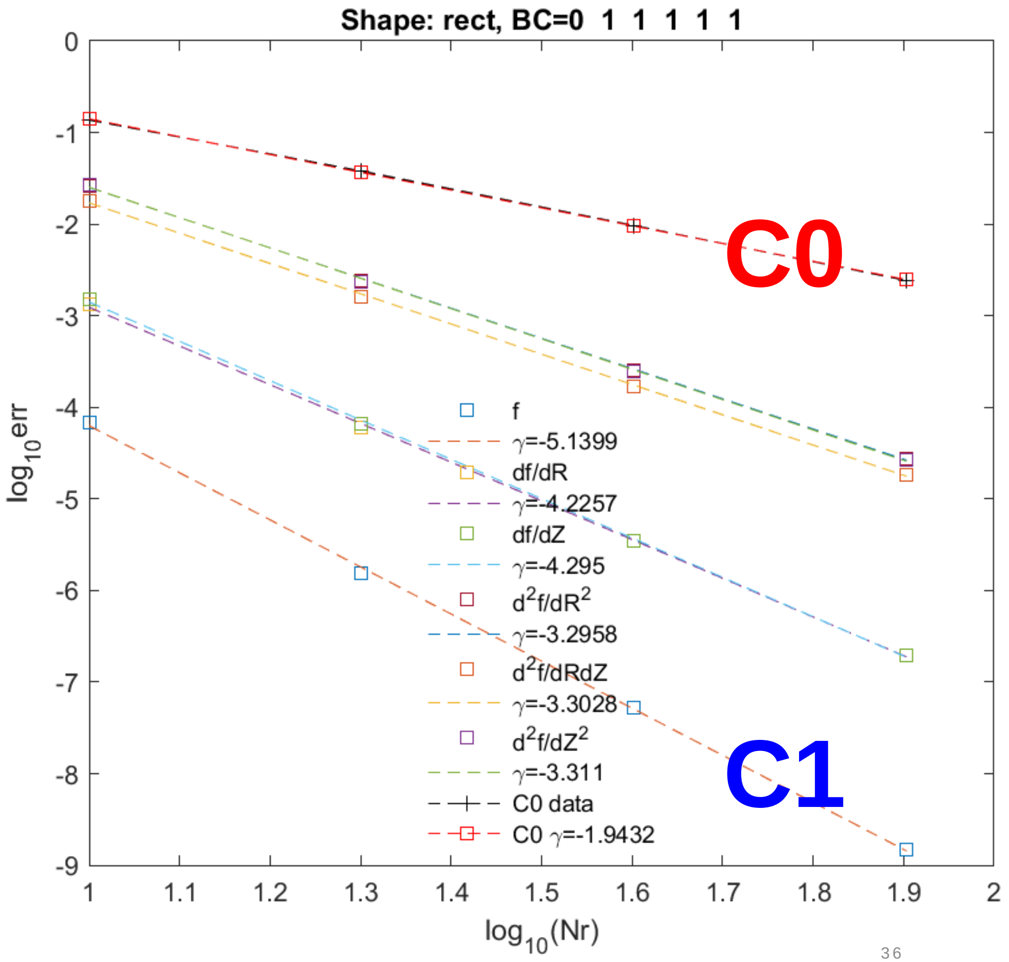

RZ plane: C1; 18 basis functions in each triangle

Quintic polynomials ($N_k(\xi,\eta) = C\xi^p\eta^q, p + q \leq 5$); C1 continuity across edges

6 degree of freedom per each node (f, $\partial f/\partial R$, $\partial f/\partial Z$, $\partial^2 f/\partial R^2$, $\partial^2 f/\partial R\partial Z$,$\partial^2 f/\partial Z^2$)

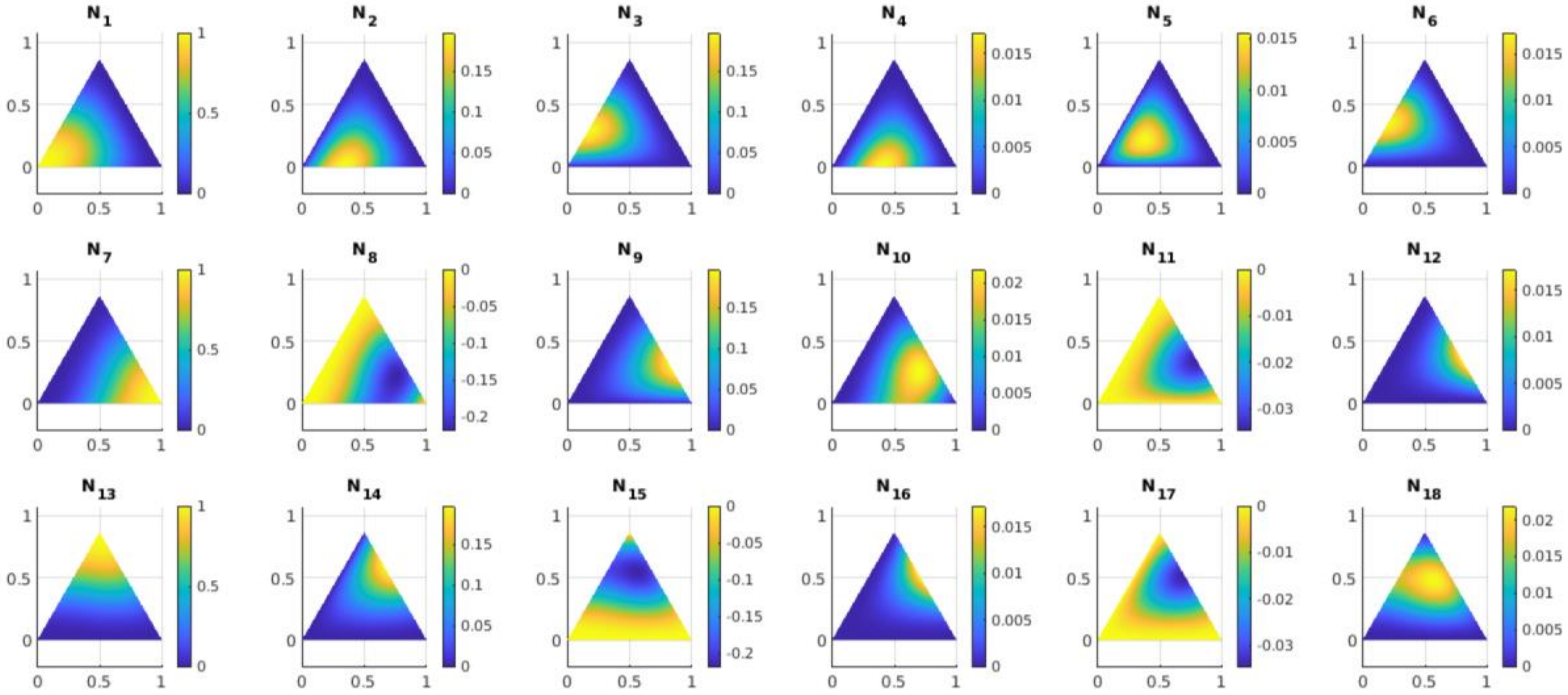

[Jardin, *J. Comput. Phys.* 200 (2004) 133]

ITG/TEM simulations with kinetic electrons and EM effects

- **Cyclone case is adopted for test**
- $n = 10$, marker #: 16e6; $\left(N_r, N_\phi\right) = (32{,}8)$; $N_\theta \sim 2\pi N_r r/a$

- d_e **increased to save computing time**
- **2D mode structure of ITG/CTEM: opposite tilting angles**
  - **Studies of flow and current generation due to turbulence merits more efforts in future; e.g., comparison with GEM results**

[X Chen, Z Lu*, H Cai* et al, PPCF 64, 115008 (2022);
X Chen, Z Lu*, H Cai*, et al, POP 28, 112303 (2021)]

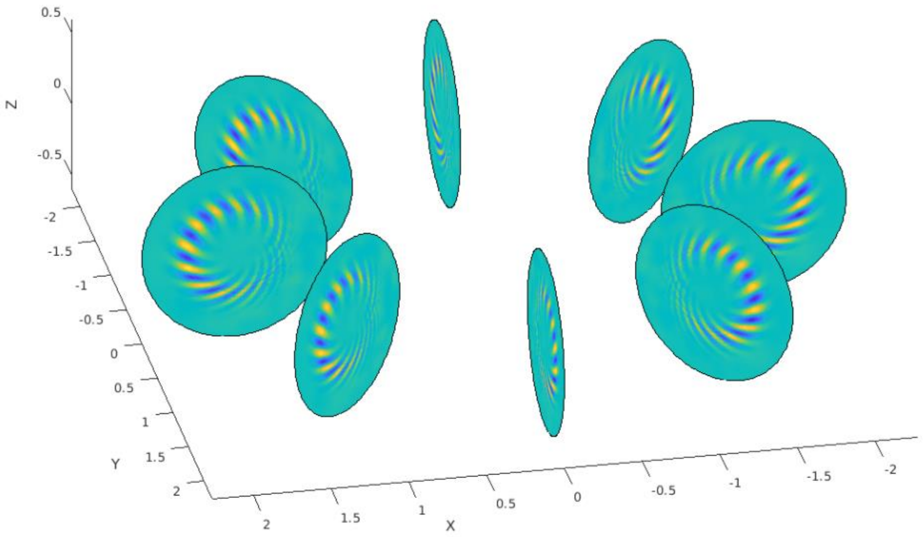

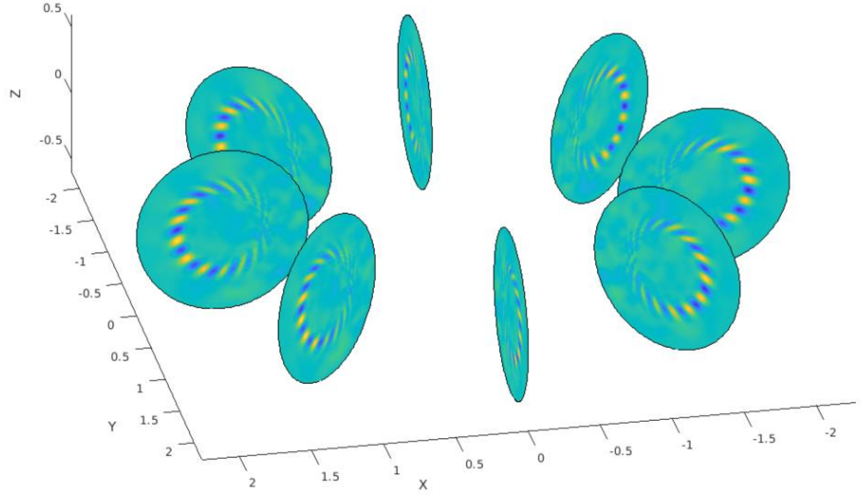

Background and motivation

(Gyro)kinetic simulations in the MHD limit reveals important physics phenomena

- Kinetic effects (finite Larmor radius/orbit width) on peeling-ballooning mode
- Energetic particle/kinetic particle effects on tearing mode, kink mode

Various numerical/physical schemes for electromagnetic gyrokinetic particle simulations

- Early treatment: fluid-like electrons (Lin01), iterative Ampere solver [Y. Chen03]
- The “cancellation” problem in the particle simulations ($p_{\|}$ or Halmitonian form) can be mitigated/eliminated by the mixed variable-pullback scheme [Hatzky19,Mishchenko14,Kleiber16]
- The implicit $v_{\|}$ or Sympletic form also shows its capability in EM gyrokinetic particle simulations [Sturdenvant21(XGC):δf, Lu21:full f]

Challenge: Full f electromagnetic particle simulations in the small electron skin depth limit

- Different concerns in full f: Higher noise level, distribution in constant of motion
- The full f mixed variable/pullback scheme has not been developed except few cases (Hager22XGC: electron skin depth $d_e = \sqrt{m_e/(\mu_0 e^2 n_0)}$ is relatively large; work here: $d_e \sim 10^{-3}$)

Reference

Hatzky, et al. Journal of Plasma Physics 85, 1 (2019)

Lanti et al. Computer Physics Communications, 251, 107072 (2019)

Kleiber, et al. Phys. Plasmas, 23, 032501 (2016)

Mishchenko, et al. Phys. Plasmas, 24, 081206 (2017)

Mishchenko, et al. Comp. Phys. Comm. 238, 194 (2019)

Bottino, et al. Plasma Phys. Control. Fusion 53, 124027 (2011)

Huysmans, et al. Nucl. Fusion 47, 659 (2007)

Hoelzl, et al. 2021 Nucl. Fusion 61 065001 (2021)

Lu, et al. Phys. Plasma, 26, 122503 (2019)

Lu, et al. Journal Compt. Phys. 440, 110384 (2021)

Lu, et al, Plasma Phys. Control. Fusion, 65, 034004(2023)